Winter 11-2-2023

A highly selective optical sensor Eu-BINAM for assessment of high sensitivity cardiac troponin tumor marker in serum of cancer patients

Ekram Hany Mohamed
The British University in Egypt, ekram.hany@bue.edu.eg

Mohamed S. Attia
Analytical Chemistry Department, Faculty of Science, Ain Shams University, Cairo, Egypt

Ahmed O. Youssef
Analytical Chemistry Department, Faculty of Science, Ain Shams University, Cairo, Egypt

Shahenda S. Ahmed
Analytical Chemistry Department, Faculty of Science, Ain Shams University, Cairo, Egypt

Spectrochimica Acta Part A: Molecular and Biomolecular Spectroscopy 300 (2023) 122887

Contents lists available at ScienceDirect

Spectrochimica Acta Part A:
Molecular and Biomolecular Spectroscopy

journal homepage: www.journals.elsevier.com/spectrochimica-acta-part-a-molecular-and-biomolecular-spectroscopy

A highly selective optical sensor Eu-BINAM for assessment of high sensitivity cardiac troponin tumor marker in serum of cancer patients

Shahenda S. Ahmed [a], Ahmed O. Youssef [a], Ekram H. Mohamed [b], Mohamed S. Attia [a,*]

[a] Analytical Chemistry Department, Faculty of Science, Ain Shams University, Cairo, Egypt
[b] Pharmaceutical Chemistry Department, Faculty of Pharmacy, British University, Cairo, Egypt

HIGHLIGHTS

- A novel and selective spectrofluorimetric technique has been applied for determination of (TNHS I).
- The technique is based on quenching of the Eu^{3+}-BINAM complex's luminescence intensity by (TNHS I).
- The synthesis and characterization of the optical sensor was performed via absorption and emission.
- The technique was effectively recruited to quantify High Sensitivity (TNHS I) in human serum samples.
- _____
  _____

GRAPHICAL ABSTRACT

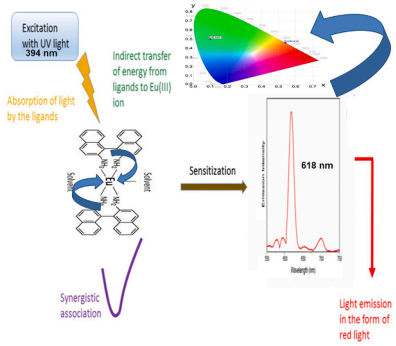

ARTICLE INFO

Keywords:
Troponin
Cardiac biomarker
Biosensor
Europium Complex
Luminescence

ABSTRACT

A novel, easy, touchy and selective spectrofluorimetric technique has been successfully applied for sensitive determination of High Sensitivity Cardiac Troponin (TNHS I) in the serum samples of patients suffering malignant tumors through the usage of optical sensor Eu^{3+}-BINAM complex. The technique is primarily based on quenching of the Eu^{3+}-BINAM complex's luminescence intensity upon introducing various concentrations of High Sensitivity Cardiac Troponin (TNHS I). The synthesis and characterization of the optical sensor was performed via absorption and emission. The sensor was also adapted to offer excitation at 394 nm in acetonitrile at pH 7.5. Concentration of High Sensitivity Cardiac Troponin (TNHS I) in serum samples was found to be proportional to the luminescence intensity quenching of the Eu^{3+}-BINAM complex, most prominently at $\lambda_{em} = 618$ nm. The limit of the dynamic range is 4.26×10^{-4} to 2 ng/mL. The limit of detection and quantitation were calculated to be 1.35 and 4.10 ng/mL, respectively. The suggested analytical approach proved its applicability, simplicity and comparatively interference- free. The technique was effectively recruited to quantify High Sensitivity Cardiac Troponin (TNHS I) in human serum samples. The proposed technique could be further extended to evaluate some biomarkers associated with malignancy related diseases in human.

* Corresponding author.

https://doi.org/10.1016/j.saa.2023.122887
Received 9 March 2023; Received in revised form 12 May 2023; Accepted 13 May 2023
Available online 19 May 2023

1. Introduction

The troponin TNHS complex which controls how striated muscles contract, is made up of three subunits, an 18 ku protein called troponin C (calcium ions binder), 37 ku protein called TNHS T (interacts to tropomyosin) securing the troponin complex attachment to the thin filament and a 24 ku protein called TNHS I which binds to actin decreasing Troponin C calcium affinity which in turn inhibits the actin-myosin interactions. Although TNHS T and troponin I are abundant in both cardiac and skeletal muscles, they are encoded by different genes in each of these two muscle types, resulting in immunologically distinct proteins.

TNHS T and cardiac troponin I specific assays are available and based on high-affinity antibodies. Since the cardiac and skeletal troponin C amino acid sequence is similar, no assays for the Troponin C have been recently developed since year 2000 [1]. TNHS (cTn) is considered to be one of the most favorable biomarker.

for assessment of patients who are suspected to suffer from an acute myocardial infarction (AMI) [2,3].

The heart can be clinically adversely affected in cancer patients, particularly some subtypes, as a result of the tumor's direct activity, its secretory outputs, or the toxicity of various oncological medications. Cardiac biomarkers were examined as readily and affordably available tools and apparatus for the early diagnosis, monitoring, or prediction of several cardiac diseases associated with malignancy [4].

There are numerous cTnI assays available in the market. These assays are not currently standardized, and investigations have revealed significant variations between methodologies. Variable antibody immunoreactivity to various circulating cTnI forms and different calibrators employed in different cTnI assays are additional factors that contribute to quantitative disparities between cTnI methods [3,5].

A variety of different analytical techniques, such as Chemiluminescence immunoassays [6,7], enzyme immunoassays [8], radioimmunoassay (RIA) [9], electrochemical Immunoassay [10], electrochemiluminescence immunosensor [11], and enzyme-linked immunosorbent assays was reported for the estimation of TNHS I [12].

However, these methods are facing many challenges to meet the expanding clinical specifications for the quick detection of TNHS I. This may be attributed to the time-consuming separations, complex label collection. Additionally, it is not feasible to detect tumor markers at ultra-low biogenic concentration using such methods. Thus there is an urge to develop novel immunoassay techniques [13].

Lanthanide probes are a non-invasive analytical tool commonly used for biological and chemical applications. Eu^{3+} complexes showed unusual luminescence properties when excited with UV light [14]. Importance of lanthanide probes increased when ***Finnish*** researchers proposed the Eu^{3+}, Tb^{3+}, Sm^{3+} and Dy^{3+} polyaminocarboxylates as luminescent sensors in time-resolved luminescent (TRL) immunoassays. Lanthanide probes' ligands must meet several chemical requirements for the probes to work properly. These qualities are: water solubility, large thermodynamic stability at physiological pHs, kinetic inertness and absorption above 330 nm to minimize destruction of live biological materials [15].

Lanthanide probes display unique fluorescence properties, including long lifetime of fluorescence, large Stokes shift and narrow emission peak. These properties are highly advantageous to develop analytical probes for receptor-ligand interactions. Many lanthanide based fluorescence studies have been developed for GPCRs, including CXCR1, [16] insulin-like family peptide receptor 2, [17] protease-activated receptor 2, [18] β2-adrenergic receptor [19] and C3a receptor [20].

Over the last two decades, lanthanide ions were increasingly used as spectroscopic probes for biological systems. The lanthanides have similar ionic radii to calcium, but by virtue of possessing a higher charge, they have a high affinity for Ca^{2+} sites on biological molecules, and a stronger binding to water molecules hence can act as either Ca^{2+} inhibitors or probes [21]. The small size of lanthanides (ionic radius) gives them the ability to replace metal ions inside protein complex such as calcium or nickel [22].

In the presented study a highly selective and straightforward analytical strategy was adopted for accurate, fast and affordable determination of cardiac troponin in cancer patients' serum. It depends on quenching the luminescence intensity of Eu-2,2 -Diamine 1,1 -Binaphthalene (Eu-BINAM) optical sensor after the addition of TNHS I with different concentrations. The newly designed sensor was fabricated and characterized via absorption and emission specifications and is customized to exhibit red luminescence in acetonitrile at λ_{em} of 618 nm when excited at 394 nm. The main mechanism through which the sensor functions is the florescence resonance energy transfer (FRET). The obtained results were statistically analysed and were found to be satisfactory. The limit of detection (LOD) of the suggested probe was 1.35 ng/mL with a correlation coefficient (r) of 0.995.

2. Experimental

2.1. Instrumentation

A double beam UV–Visible Spectrophotometer (Thermo scientific Evolution 300) equipped with a xenon flash lamp having a spectral range of 190–1100 nm as a light source. A spectrofluorometer (Edinburgh Instruments FS5) having a spectral range up to 1650 nm and fluorescence lifetimes down to 25 ps. A pH meter (Jenway 3040). A Daihan Scientific centrifuge device (CF-10 model).

2.2. Materials

Ethanol, Acetonitrile, Dimethyl Sulfoxide (DMSO), and Dimethyl Formamide (DMF), Europium (III) nitrate, and 2,2 -Diamine-1,1 Binaphthalene (BINAM) were purchased from Sigma Aldrich. High Sensitivity Troponin (TNHS I) was purchased from BioMérieux. Human serum samples were collected from Raba'a El-Adwyea hospital (Nasr city, Egypt). The procedure for collecting human specimens was carried out in compliance with World Health Organization (WHO) approval. The ethics committee at Ain Shams University gave its approval for all tests to be carried out in accordance with the guidelines established by the "Ministry of Health and Population, Egypt." The humans participating in this study provided informed consents.

2.3. Standard solutions

2.3.1. Stock solutions

In a 10-mL volumetric flask, a stock solution of 1.0×10^{-2} mol L^{-1} Eu $(NO_3)_3$ was prepared in ethanol. In another 10-mL volumetric flask, a stock solution of 2×10^{-2} mol L^{-1} 2,2 -Diamine-1,1 Binaphthalene (BINAM) was prepared using ethanol. For TNHS I, its stock solution was prepared through accurately transferring 0.5 gm in 2 mL deionized water.

2.3.2. Working solution

$Eu(NO_3)_3$ and BINAM working solutions were separately prepared with concentrations of 1.0×10^{-4} mol L^{-1} and 2.0×10^{-4} mol L^{-1} respectively through appropriate dilutions from their respective stock solutions. Eu^{3+}-BINAM complex working solution was prepared by transferring accurate predetermined aliquots, from the separate working solutions previously prepared, into a 25-mL volumetric flask and the volume was adjusted to the mark using acetonitrile to obtain a final concentration of (1.0×10^{-4} mol L^{-1}). To prepare TNHS I working solution, 100 μL from its corresponding stock solution was accurately added to 10 mL water. From the later working solution, a calibration set for TNHS I was prepared. When not in use, all stock and working solutions were kept at 2–8 °C.

2.4. General procedure

2.4.1. Preparation of standard solution

The following solutions were added to a 25-mL volumetric flask in that order; 0.25 mL of 1.0×10^{-2} mol L^{-1} $Eu(NO_3)_3$ and 0.50 mL of 1.0×10^{-2} mol L^{-1} 2,2 -Diamine-1,1 Binaphthalene (BINAM) Fig. 1(a), then the mixture was diluted with acetonitrile to the mark to finally obtain 1.0×10^{-4} mol L^{-1} of $Eu(NO_3)_3$ and 2.0×10^{-4} mol L^{-1} of BINAM Fig. 1 (b). The stated procedures were followed for performing the subsequent measurements of absorption and emission spectra as well as pH and solvent effects. The intensity of luminescence was recorded at $\lambda_{ex}/\lambda_{em}$ = 394/618 nm.

2.4.2. Calibration curve:

A 1-mL of optical probe Eu^{3+}-BINAM was thoroughly mixed with each standard solution of TNHS I with different concentrations, as previously detailed, in the spectro-photometer cell. The luminescence spectra were then recorded at the chosen λ_{ex} = 394 nm.

2.4.3. Determination of TNHS in serum samples

Blood samples were collected from 13 volunteers and were centrifuged for 15 min at 4000 rpm to separate interfering proteins. 5 μL of each serum sample was added to 1 mL of Eu^{3+}-BINAM sensor. The luminescence intensity was measured before and after addition of Eu^{3+}-BINAM optical sensor. The concentration of TNHS I was determined from the corresponding calibration graph.

3. Results and discussion

3.1. Absorption spectra

The absorption spectra of Eu^{3+}-BINAM complex is illustrated in Fig. 2. Spectrum 1 represents the absorption spectrum of the ligand BINAM exhibiting a prominent peak at 235 nm owing to the $\pi \rightarrow \pi^*$ transition in the rings of BINAM ligand. While spectrum 2 represents the red shift, by 3 nm, which occurs upon BINAM ligand complexation with Eu^{3+} ion (1.0×10^{-4} mol L^{-1}) indicating formation of a stable complex between both of them. Finally, spectrum (3) indicating a higher absorption after addition of 3.72×10^{-3} ng/mL of TNHS I to Eu^{3+}-BINAM complex.

3.2. Emission spectra and the lifetime of Eu^{3+}-BINAM sensor luminescence:

The luminescence emission spectra of Eu^{3+}-BINAM complex is shown in Fig. 3. The intensity of the significant Eu^{3+} ion peaks appear at $^5D_0 \rightarrow {}^7F_0$ = 590 nm; $^5D_0 \rightarrow {}^7F_1$ = 590 nm; $^5D_0 \rightarrow {}^7F_2$ = 618 nm; $^5D_0 \rightarrow {}^7F_3$ = 650 nm; $^5D_0 \rightarrow {}^7F_4$ = 690 nm and $^5D_0 \rightarrow {}^7F_5$ = 710 nm.

3.3. The luminescence life time of Eu^{3+} ion complexes

The luminescence techniques have a significant role as a tool for exploring Eu^{3+} coordination chemistry [23,22,24–31]. Excited lanthanide both ions and complexes have different luminescence lifetimes that could vary from milliseconds such as Yb and Nd to microseconds as Eu and Tb. This relatively long emission lifetime is considered appealing from an analytical perspective where it permits time gating procedures to be implemented facilitating the discrimination between lanthanide luminescence and the shorter lived backgrounds, last up to sub-microseconds, which is typically present in most of analytical and biological systems. Eu^{3+} is counted as one of the 2 longest-lived and most widely investigated emitting lanthanide ions. It owes a luminescent $^5D_0$ excited state with energy estimated around 17200 cm^{-1} [23].

The normalized time-resolved decay spectra of the Eu^{3+}-BINAM sensor emission is shown in Fig. 4, the lifetime of the $^5\mathbf{D_0}$ excited state is 9.68×10^3 μS at λ_{em} = 618 nm which is a considerable long lifetime value. The experimental data are fitted by mono-exponential decay which is the best fit due to the high signal to noise ratio.

The influence of TNHS I concentration on the luminescence intensity of the Eu^{3+}-BINAM was studied under the optimum experimental conditions. The results are shown in Fig. 5. After the addition of different concentrations of TNHS I (4.26×10^{-4}–2 ng/mL) into the Eu^{3+}-BINAM complex, characteristic peaks of Eu^{3+} ion, especially the peak at λ_{em} = 618 nm ($^5D_0 \rightarrow {}^7F_2$) of Eu^{3+} were quenched by increasing the concentration of TNHS I up to 27 ng/mL because TNHS I quenches the excited state of the Eu^{3+}-BINAM by the energy transfer from the optical sensor to the TNHS I.

3.4. Effect of experimental variables

3.4.1. Solvent effect

Following the above established conditions, the impact of different solvents on the luminescence intensity of solutions, containing (1.0×10^{-4} mol L^{-1}) Eu – (2.0×10^{-4} mol L^{-1}) BINAM, was investigated. The resulting data revealed the enhancement of Eu-BINAM complex emission in acetonitrile as displayed in Fig. 6. The intensity of complex luminescence in acetonitrile is stronger than that in Dimethyl Formamide (DMF), Dimethyl Sulfoxide (DMSO), water and ethanol. This can be due to Eu^{3+}-BINAM complex anhydrous solvates formation which introduce solvent molecules in Eu^{3+}-BINAM first coordination sphere, thus enhancing the intensity of all transitions, $^5D_0 \rightarrow {}^7F_0$ = 590 nm; $^5D_0 \rightarrow {}^7F_1$ = 590 nm; $^5D_0 \rightarrow {}^7F_2$ = 618 nm; $^5D_0 \rightarrow {}^7F_3$ = 650 nm; $^5D_0 \rightarrow {}^7F_4$ = 690 nm and $^5D_0 \rightarrow {}^7F_5$ = 710 nm, the $^5D_0 \rightarrow {}^7F_2$ transition in Eu^{3+}, in specific [32-34]. The peaks at 592 ($^5D_0$–$^7F_1$), 700 ($^5D_0$–$^7F_4$) and 618 nm ($^5D_0$–$^7F_2$) are ascribed to the magnetic dipole and electric dipole transitions, respectively. The strong peak at 618 nm, which corresponds the $^5D_0$–$^7F_2$ transition, can be attributed to the allowed electric dipole transition with inversion antisymmetry (Fig. 6, lines 1, 2 and 3) [35–38].

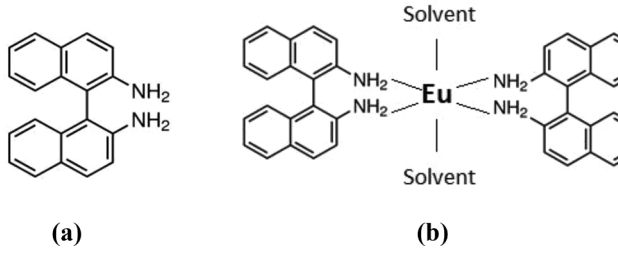

Fig. 1. (a) Structure of BINAM ligand and (b) Structure of Eu^{3+}-BINAM complex (1:2).

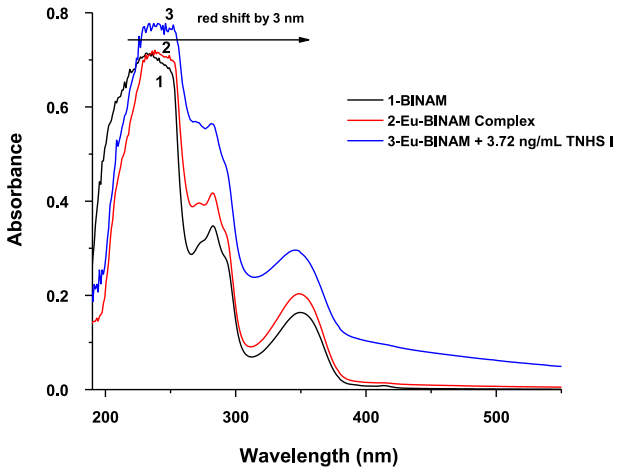

Fig. 2. The absorption spectra of BINAM ligand, Eu^{3+}BINAM complex and Eu^{3+}-BINAM complex + TNHS I.

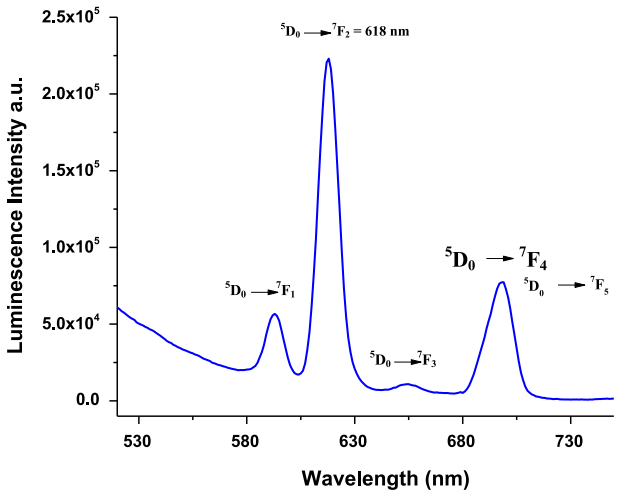

Fig. 3. Emission spectra of Eu^{3+}-BINAM sensor at 394 nm excitation.

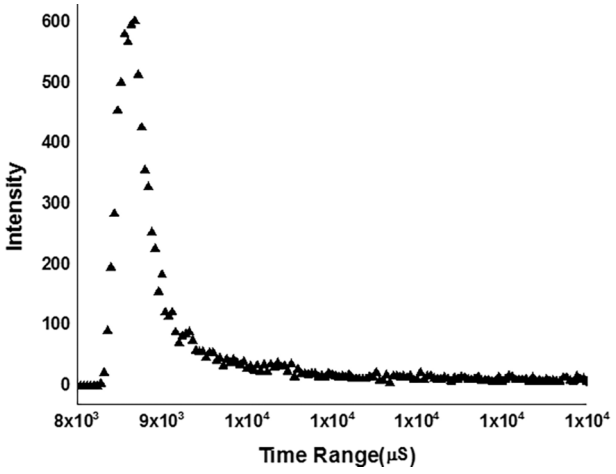

Fig. 4. Normalized time-resolved decay spectra of Eu^{3+}-BINAM sensor.

The peak at 592 nm, which corresponds to the $[5]D_0-{}^7F_1$ transition, is due to the allowed magnetic dipole transition. According to the Laporte selection rule (equal parity), if an Eu^{3+} ion is situated in a symmetry center, the electric dipole transitions between the $4f^6$ levels are strictly forbidden, whereas the magnetic dipole transition is still possible. On the other hand, the electric dipole transition intensity should be stronger than the magnetic dipole transition intensity in an asymmetric environment, as stated by the Judd–Ofelt theory. The intensity at 618 nm (electric dipole transition) is stronger than that at 592 and 700 nm (magnetic dipole transitions), which signifies that Eu^{3+} occupied sites have low inversion symmetry or asymmetric environment. The intensity ratio of the $^5D_0-{}^7F_2$ to $^5D_0-{}^7F_1$ and $^5D_0-{}^7F_2$ to $^5D_0-{}^7F_4$ transitions (618/592 and 618/700 nm), called the symmetry ratio, can provide information about the structural quality of the material. As presented in Fig. 6, the symmetry ratios of Eu–BINAM (DMSO, line 4) sample are from 0.97 to 0.72, due to the increase in the symmetry for the Eu^{3+}-occupying sites.

3.4.2. *pH effect*

The apparent pH of the media has a significant impact on the Eu^{3+}-

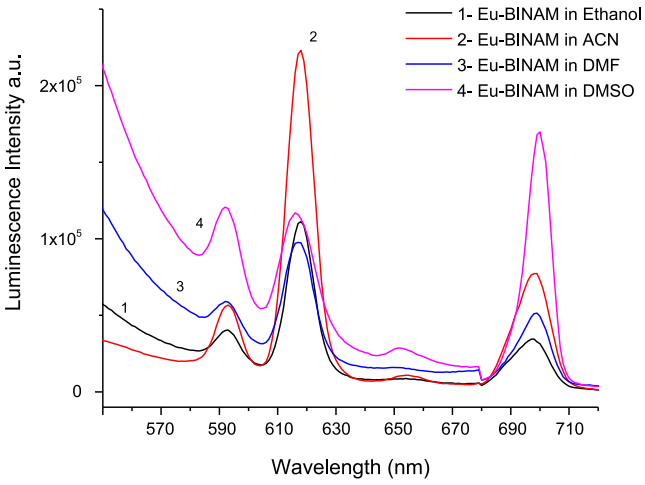

Fig. 6. Luminescence emission spectra of Eu^{3+}-BINAM complex in the presence of different solvents.

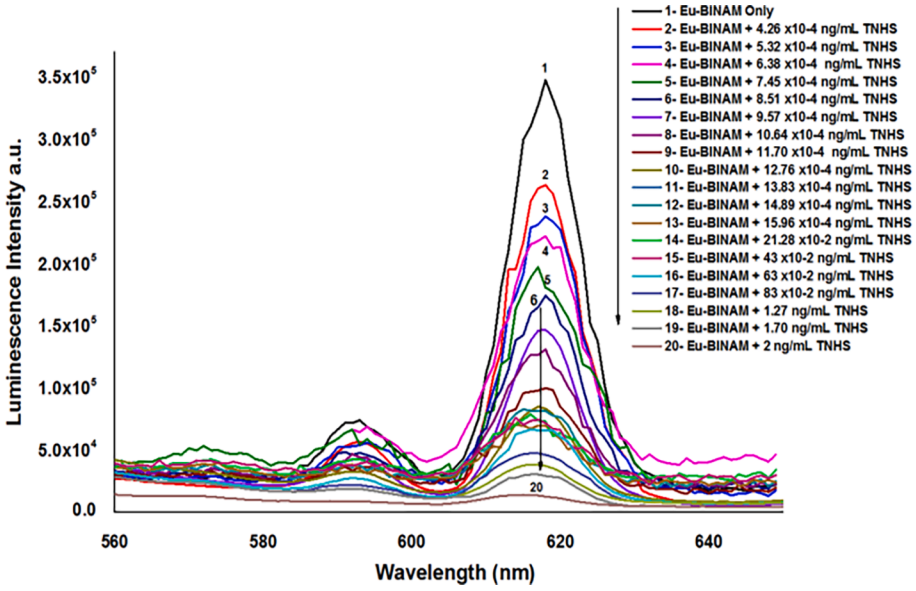

Fig. 5. Luminescence emission spectra of Eu^{3+}-BINAM complex in the presence of different concentrations of TNHS I in acetonitrile at λ_{ex} = 394 nm and pH = 7.5.

BINAM complex luminescence intensity. 0.1 mol L^{-1} of both NaOH and HCl solutions were used to adjust the pH. The highest intensity was recorded at the apparent pH value of 7.5 at $\lambda_{em} = 618$ nm, which was considered to be the optimum pH and it was suitable for the **TNHS I** assessment which is soluble at pH of 7.5, Fig. 7. The luminescence intensity of Eu-2,2′-Diamine-1,1′-Binaphthalene complex in acetonitrile is affected by pH. The luminescence intensity is highest at pH 7.5 and decreases as the pH increases or decreases. This is due to the fact that the Eu^{3+} ion has a higher affinity for oxygenated ligands than for unoxygenated ligands. At pH 7.5, the solution is neutral, and the Eu^{3+} ion is mostly coordinated by unoxygenated ligands. As the pH increases, the solution becomes more basic, and the Eu^{3+} ion is increasingly coordinated by oxygenated ligands. This coordination of oxygenated ligands decreases the luminescence intensity of the Eu^{3+} ion. As the pH decreases, the solution becomes more acidic, and the Eu^{3+} ion is increasingly coordinated by (H^+) water molecules. This coordination of water molecules also decreases the luminescence intensity of the Eu^{3+} ion.

Eu^{3+}-BINAM complex emission spectra in different molar ratios are shown in Fig. 8. The best of molar ratio is (M:L) (1:2) Eu^{3+}-BINAM with high intensity. The other molar ratios (M:L) (1:3) and (1:4) mainly show steric hindrance due to addition of extra bulky BINAM ligand which may cause crowding around Eu^{3+} and hence weakness of bonds between BINAM and Eu^{3+} leading to lower stability of (1:3) and (1:4) complexes.

4. Analytical performance

4.1. Analytical parameters

4.1.1. Dynamic range

The effect of the concentration of the TNHS I on the fluorescence intensity of the optical sensor Eu^{3+}-BINAM complex at $\lambda_{em} = 618$ nm is shown in Fig. 9. The calibration curve shown in Fig. 9 which was obtained by applying the Stern-Völmer [39] plot at $\lambda_{em} = 618$ nm:

Stern-Völmer plot:

$$\frac{F_0}{F} - = K_s[Q]$$

where F_o and F are the intensities of luminescence of optical sensor in absence and presence of TNHS I, respectively, Q is the TNHS I concentration and K_s is Stern-Völmer constant which is determined from the slope of the plot of [$F_o/F - 1$] against TNHS I and equals to 5.33 and $C_o = 1/K_{sv} = 0.187$ ng/mL, and R_o (critical transfer distance, which is the average distance between TNHS I and the ionophore) indicating the probability of intermolecular energy transfer is just equal to the sum of probabilities for all the de-excitation processes of the donor excited state (mechanism of quenching is electron transfer process from ionophore to TNHS I) and was found to be $7.35/(C_o)^{-1/3} = 4.20$ Å ($R_o < 10$ Å),] this means that the quenching is carried out by (**dynamic**) collision mechanism in which the electron transfer from the optical sensor to the quencher (TNHS I) [40–58].

From the plot of [(F_0/F)-1] against [TNHS I], the fluorescence intensity at 618 nm is decreased linearly with the concentrations of TNHS I over the range 4.26×10^{-4} to 2 ng/mL with a correlation coefficient of 0.995. According to ICH recommendations [59,60], the limit of detection (LOD) and quantitation (LOQ) were calculated using the relations: LOD = 3.3S/b (equals to 1.35 ng/mL) and LOQ = 10S/b (equals to 4.10 ng/mL), where S is the standard deviation of blank luminescence intensity and b is the calibration plot slope. These results are tabulated in Table 1. The comparison of the proposed optical sensor for the determination of TNHS I with other published methods [61–69], indicate that the developed method has good stability, lower limit of detection (1.35 ng/mL) and wide linear range of application (4.26×10^{-4} to 2 ng/mL).

4.2. Selectivity

The method's selectivity and validity were examined through investigating the influence of potential interfering substances on the emission spectra Eu^{3+}-BINAM upon the addition of TNHS I (2.1 ng/mL). The interfering substances included biotin (200 ng/mL), bilirubin (1 mg/mL), hemoglobin (2 mg/mL), ascorbic acid (20 mg/dL), cholesterol (8 mg/mL), albumin (0.7 g/L) and triglyceride (12.5 mg/mL). all the interfering substances exhibited no significant effect on the emission intensity of Eu^{3+}-BINAM sensor, Fig. 10.

Eu-2,2′-Diamine-1,1′-Binaphthalene complex (Eu- **BINAM**) is a lanthanide chelator that has been shown to bind to troponin I (TnI) with high affinity. The binding of Eu- **BINAM** to TnI is thought to be due to the fact that TnI has a high affinity for metal ions. TnI also has a number of residues that are capable of binding Eu^{3+} ions. These residues include aspartate, glutamate, and histidine. The binding of Eu- **BINAM** to TnI is selective for TnI over troponin C (TnC) and troponin T (TnT). This is due to the fact that TnI has a higher affinity for Eu^{3+} ions than TnC and TnT. The selectivity of Eu- **BINAM** for TnI is important for the use of this chelator in biomedical applications. For example, Eu-DOTA could be used to image or monitor TnI function in vivo. It is important to note that the selectivity of Eu- **BINAM** for different troponins is not absolute. In some cases, Eu- **BINAM** may bind to TnC and TnT, but this binding is much weaker than its binding to TnI. The selectivity of Eu- **BINAM** for different troponins is due to the different amino acid sequences of these

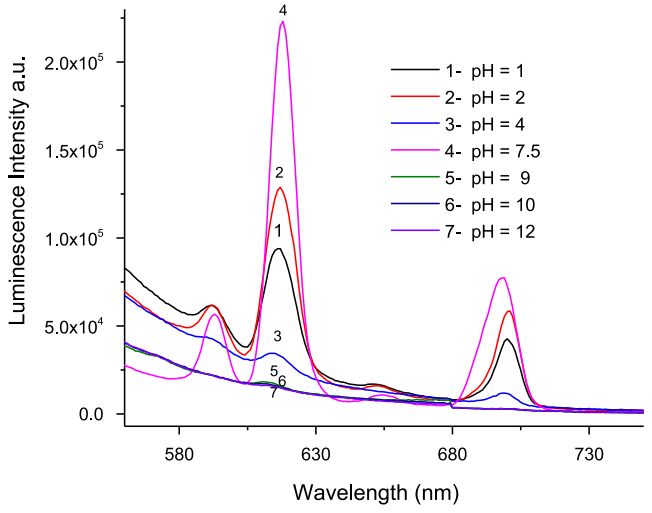

Fig. 7. Luminescence emission spectra of Eu^{3+}-BINAM complex in acetonitrile at $\lambda_{ex} = 394$ nm in different pH.

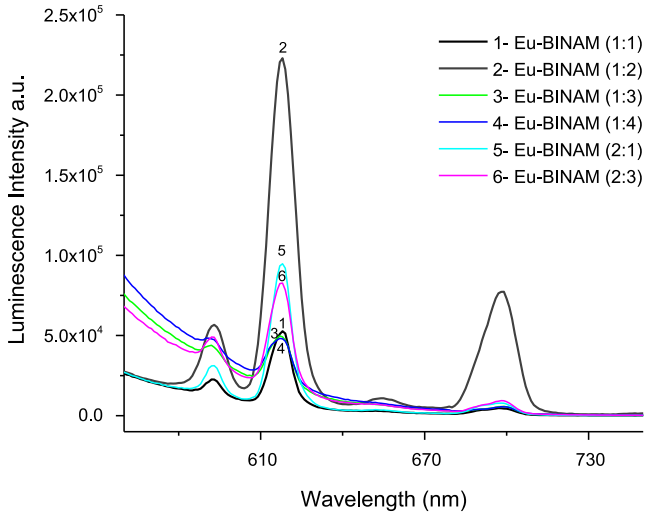

Fig. 8. Emission spectra of different molar ratio of Eu^{3+}-BINAM complex.

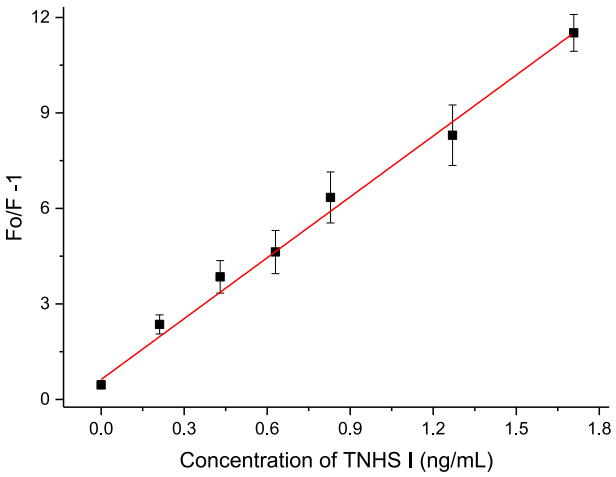

Fig. 9. Stern-Völmer plot (Fo/F−1) Vs concentration of TNHS I (ng/mL).

Table 1
The regression parameters for Eu^{n+}-BINAM complex sensor:

Parameter	Value
λ_{em} (nm)	618
Liner range (ng/mL)	4.26×10^{-4} to 2
LOD (ng/mL)	1.35
LOQ (ng/mL)	4.10
Regression equation, Y*	Y = a + bX
Intercept (a)	1.67
Slope (b)	5.33
SD	2.19
Variance (Sa^2)	4.79
Regression coefficient (r^2)	0.995

Where Y is fluorescence intensity, X is concentration in ng/mL.

proteins. TnI has a higher affinity for Eu^{3+} ions than TnC and TnT because it has a higher number of residues that are capable of binding Eu^{3+} ions. These residues include aspartate, glutamate, and histidine. The selectivity of Eu- **BINAM** for different troponins is also due to the different structures of these proteins. TnI has a more open structure than TnC and TnT, which allows Eu^{3+} ions to bind more easily.

4.3. Application to formulations

The proposed optical method was used to determine the TNHS I concentration in 13 serum samples from healthy human subjects in order to assess its applicability. The findings presented in Table 2 demonstrate that the adopted technique was found to be successful and valid for identifying TNHS I in serum samples. It was obvious, from the obtained average value of TNHS I concentration in serum samples by the newly proposed method (26.85 ± 0.62 ng/mL) in comparison with that obtained from the standard method (27 ng/mL), the method excellence with respect to accuracy and precision. The average recovery and **R.S.D.** for the serum sample using the proposed optical sensor was found to be (99.49 ± 3.2) % were also presented in Table 2 for comparison and show a good correlation with those of reference method [70], and with the label claimed.

4.4. Recovery study

For further assessment of the method's accuracy, recovery experiments were performed to determine the extent of agreement between the standard concentrations and known added concentrations to the sample. The percentage recovery values in Table 2 ranged from 96.29 to 102.7 % with relative standard deviation **(RSD)** ranging from 0.089 to 6.2 % for serum samples. The results approaching 100% assured the good accuracy of the proposed method.

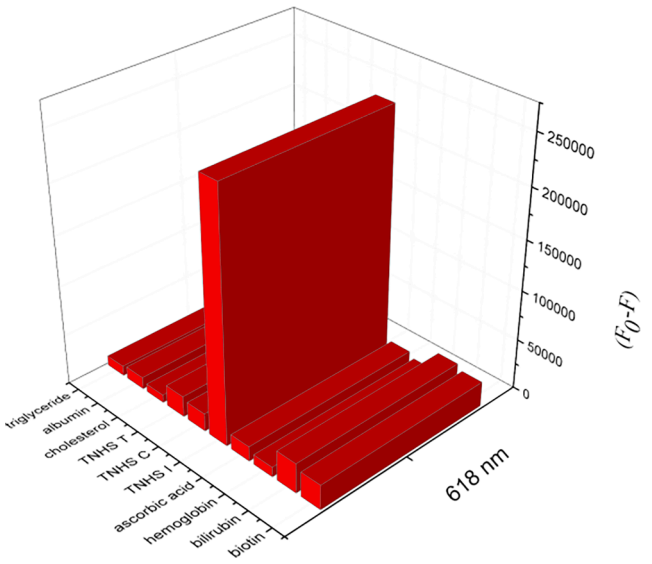

Fig. 10. Effect of interfering species on the selectivity of Eu-BINAM sensor for Troponin I.

4.5. Precision and accuracy study

For precision computation, the assays were performed in triplicates within the same day and on three different days for determination of method's repeatability and intermediate precision, respectively. The average percentage relative standard deviation **(%RSD)** values were calculated and found to be ≤0.5–6.2 and ≤ 0.089–3.2 for intra-day and inter-day precisions, respectively for the serum samples indicating the high precision of the proposed method. Accuracy of the proposed method was evaluated as percentage relative error (%RE) between the measured mean concentrations and the taken concentrations of TNHS I. %RE was calculated at each concentration and the obtained results were summarized in Table 2**.** Percent relative error **(%RE)** were found to be ≤(0.31–3.7) (intraday) and ≤(0.20–1.35) (inter-day) for the serum samples demonstrating the high accuracy of the proposed method.

5. Conclusion

Eu^{3+}-BINAM complex exhibited characteristic peaks which are significantly quenched in the presence of TNHS I at $\lambda_{ex}/\lambda_{em}$ = 394/618 nm owing to the energy transfer from the Eu^{3+}-BINAM complex. The method was found to be reliable and applicable for determination of TNHS I in serum with high accuracy and precision.

%RE, Percent relative error. %RE = [(concentration proposed- concentration known)/concentration known] × 100, %RSD, relative standard deviation. %RSD = [S/(average measurements)] × 100, and ± CL, Confidence limits: CL = $tS/n^{(1/2)}$. (The tabulated value of t is 4.303, at the 95% confidence level; S = standard deviation and n = number of measurements).

Declaration of Competing Interest

The authors declare that they have no known competing financial interests or personal relationships that could have appeared to influence the work reported in this paper.

Data availability

No data was used for the research described in the article.

Table 2
Evaluation of intra-day and inter-day accuracy and precision:

Sample	Standard method Average ng/mL	Proposed method									
		Intra-day accuracy and precision (n = 3)					Inter-day accuracy and precision (n = 3)				
		Average found		%RE	Average Recovery	%RSD	Average found		%RE	Average Recovery	%RSD
		ng/mL	± CL				ng/mL	± CL			
Patient (1)	27	26.80	± 0.945	0.74	99.26	1.4	26.90	± 0.302	0.37	99.63	0.45
Patient (2)	22	22.20	± 0.645	0.90	100.91	1.2	21.95	± 0.216	0.22	99.77	0.39
Patient (3)	19	19.15	± 0.322	0.79	100.79	0.7	18.96	± 0.042	0.21	100.79	0.089
Patient (4)	16	15.95	± 0.967	0.31	99.69	2.4	16.10	± 0.124	0.625	100.63	0.31
Patient (5)	10	10.05	± 0.124	0.50	100.5	0.5	10.10	± 0.327	1	101	1.30
Patient (6)	5	5.10	± 0.087	2	102	0.68	5.01	± 0.025	0.20	100.20	0.19
Patient (7)	1.54	1.50	± 0.139	2.50	97.40	3.7	1.55	± 0.042	0.65	100.65	1.10
Patient (8)	1.40	1.41	± 0.049	0.71	100.70	1.4	1.39	± 0.11	0.71	99.29	3.20
Patient (9)	1	0.98	± 0.149	2	98	6.2	1.01	± 0.0248	1	101	0.99
Patient (10)	0.49	0.48	± 0.0124	2	97.96	1	0.485	± 0.011	1.02	98.98	0.88
Patient (11)	0.37	0.38	± 0.021	2.7	102.70	2.2	0.365	± 0.021	1.35	98.65	2.40
Patient (12)	0. 27	0.26	± 0.012	3.7	96.29	1.9	0.273	± 0.011	1.11	101	1.61
Patient (13)	0.12	0.118	± 0.0064	1.6	98.33	2.24	0.121	± 0.004	0.83	100.8	1.32

References

[1] E.M. Antman, Decision making with cardiac troponin tests, N. Engl. J. Med. 346 (2002) 2079–2082.
[2] S. Jaffea, J. Ordonez-Llanos, Rev. Esp Cardiol (Eng Ed) (2013).
[3] X.u. Ru-Yi, X.-F. Zhu, Y.e. Yang, P. Ye, High-sensitive cardiac troponin T, J. Geriatr. Cardiol. 10 (2013) 102–109.
[4] G.C. Semeraro, C.M. Cipolla, D.M. Cardinale, Role of cardiac biomarkers in cancer patients, Cancers 13 (2021) 5426.
[5] K. Thygesen, J. Mair, H. Katus, et al., Recommendations for the use of cardiac troponin measurement in acute cardiac care, Eur. Heart J. 31 (2010) 2197–2204.
[6] J. Wang, Y. Fang, P. Li et al., Evaluation of a newly developed chemiluminescence immunoassay for detecting cardiac troponin T, J. Clin. Lab Anal. 32 (2018) e22311.
[7] C.h. Zong, D. Zhang, H. Yang, S.h. Wang, M. Chu, P. Li, Chemiluminescence immunoassay for cardiac troponin T by using silver nanoparticles functionalized with hemin/G-quadruplex DNAzyme on a glass chip array, Microchim. Acta 184 (2017) 3197–3204.
[8] K. Suetomi, K. Takahama, A sandwich enzyme immunoassay for cardiac troponin I, Nihon Hoigaku Zasshi 49 (1) (1995) 26–32.
[9] B. Cummins, M.L. Auckland, P. Cummins, Cardiac-specific troponin-I radioimmunoassay in the diagnosis of acute myocardial infarction, Am. Heart J. 113 (6) (1987) 1333–1344.
[10] S. Feng, M. Yan, Y. Xue, J. Huang, X. Yang, Electrochemical immunosensor for cardiac troponin I detection based on covalent organic framework and enzyme-catalyzed signal amplification, Anal. Chem. 93 (40) (2022) 13572–13579.
[11] M. Tang, Z. Zhou, L. Shangguan, F. Zhao, S. Liu, Electrochemiluminescent detection of cardiac troponin I by using soybean peroxidase labeled-antibody as signal amplifier, Talanta 180 (2018) 47–53.
[12] H.A. Katus, A. Remppis, S. Looser, K. Hallermeier, T.h. Scheffold, W. Kübler, Enzyme linked immuno assay of cardiac troponin T for the detection of acute myocardial infarction in patients, Rapid Commun. 21 (12) (1989) P1349–P1353.
[13] W. Wensheng, S.h. Li, Z. Guannan, H. Jianxin, M. Zhiqiang, Int. J. Electrochem. Sci. 12 (2017) 10791.
[14] E. Soini, T. Lövgren, C.B. Reimer, Time-resolved fluorescence of lanthanide probes and applications in biotechnology, CRC Crit. Rev. Anal. Chem. 18 (2) (1987) 105–154.
[15] J.C.G. Bünzli, Lanthanide luminescence for biomedical analyses and imaging, Chem. Rev. 110 (5) (2010) 2729–2755.
[16] J. Inglese, P. Samama, S. Patel, J. Burbaum, I.L. Stroke, K.C. Appell, Chemokine receptor- ligand interactions measured using time-resolved fluorescence, Biochemistry 24; 37 (8) (1998) 2372–2377.
[17] F. Shabanpoor, R.A. Hughes, R.A.D. Bathgate, S. Zhang, D.B. Scanlon, F. Lin, et al., Solid-phase synthesis of europium labaled human INSL3 as a novel probe for the study of ligand receptor interactions, Bioconjug. Chem. 19 (7) (2008) 1456–1463.
[18] J. Hoffman, A. N. Flynn, D. V. Tillu, Z. Zhang, R. Patek, T.J. Price et al., Lanthanide labeling of a potent protease activated receptor-2 agonist for time-resolved fluorescence analysis, 2012, Vol. 23, Issue 10 : 2098-2104.
[19] E. Martikkala, M. Lehmusto, M. Lilja, A. Rozwandowicz-Jansen, J. Lunden, T. Tomohiro, P. Hanninen et al., 15; 392 (2) (2009) 103–109.
[20] A. Dantas de Araujo, C. Wu, K.C. Wu, R.C. Reid, T. Durek, J. Lim, D.P. Fairlie, Europium labeled synthetic C3a protein as a novel fluorescent probe for human complement C3a receptor, Bioconjug. Chem. 21; 28 (6) (2017) 1669–1676.
[21] S.P. Fricker, The therapeutic application of lanthanides, Chem. Soc. Rev. 35 (2006) 524–533.
[22] J.C.G. Bünzli, G.R. Choppin, Lanthanide Probes In Life, Chemical and Earth Sciences: Theory and Practise, Elsevier, Amsterdam, 1989.
[23] W. Horrocks, D.R. Sudnick, J. Am. Chem. Soc. 101 (1979) 334.
[24] J.L. Kropp, M.W. Windsor, J. Phys. Chem. 71 (1967) 477.
[25] Y. Haas, G. Stein, J. Phys. Chem. 75 (1971) 3677.
[26] Y. Haas, G. Stein, J. Phys. Chem. 75 (1971) 3668.
[27] P.P. Barthelemy, G.R. Choppin, Inorg. Chem. 28 (1989) 3354.
[28] G.R. Choppin, D.R. Peterman, Coord. Chem. Rev. 174 (1998) 283.
[29] D. Parker, Coord. Chem. Rev. 205 (2000) 109.
[30] M.H. Keefe, K.D. Benkstein, J.T. Hupp, Coord. Chem. Rev. 205 (2000) 201.
[31] A. Nehlig, M. Elhabiri, I. Billard, A.M. Albrecht-Gary, K. Lützenkirchen, Photoexcitat-ion of europium (III) in various electrolytes: Dependence of the luminescence lifetime on the type of salts and the ionic strength, Radiochim. Acta 91 (2003) 37–43.
[32] M.S. Attia, S.A. Elsaadany, K.A. Ahmed, M.M. El-Molla, S.A. Abdel-MottalebM, J. Fluoresce. 25 (2015) 119–125.
[33] M. S. Attia, M.S.A. Abdel-Mottaleb, Polymer-doped nano-optical sensors for pharmaceutical analysis, in: V.K. Thakur, M.K. Thakur (Eds.), Handbook of Polymers for Pharmaceutical Technologies: Processing and Applications, vol. 2, John Wiley & Sons, Inc., Hoboken, NJ, USA, 2015, Ch.14.
[34] M.S. Attia, A.E.M. Mekky, Z.A. Khan, M.S.A. AbdelMottaleb, Nano-optical Biosensors for Assessment of Food Contaminants, in: V. Thakur, M. Thakur (Eds.), Functional Biopolymers, Springer Series on Polymer and Composite Materials. Springer, Cham, 2018.
[35] W. Chen, A.G. Joly, C.M. Kowalchuk, J.O. Malm, Y.N. Huang, J.O. Bovin, Structure, luminescence, and dynamics of Eu_2O_3 nanoparticles in MCM-41, J. Phys. Chem. B 106 (2002) 7034–7041.
[36] A.K. Parchur, R.S. Ningthoujam, Behaviour of electric and magnetic dipole transitions of Eu^{3+}, 5_D0 -$_7$F0 and Eu−O charge transfer band in ^{L}i+ co-doped $Y_PO4:^{Eu}3+$, RSC Adv. 2 (2012) 10859–10868.
[37] S.K. Gupta, C. Reghukumar, R.M. Kadam, Eu^{3+} local site analysis and emission characteristics of novel $Nd_2Zr_2O_7$: Eu phosphor: insight into the effect of europium concentration on its photoluminescence properties, RSC Adv. 6 (2016) 53614–53624.
[38] J. Zhou, L. Xie, J. Zhong, H. Liang, J. Zhang, M. Wu, Site occupancy and luminescence properties of Eu^{3+} in double salt silicate $Na_3LuSi_3O_9$, Opt. Mater. Express 8 (2018) 736–743.
[39] O. Stern, M. Volmer, Über die abklingzeit der fluoreszenz, Z. Phys. 20 (1919) 183–188.
[40] M.S. Attia, M.H. Khalil, M.S.A. Abdel-Mottaleb, M.B. Lukyanova, Y.A. Alekseenko, B. Lukyanov, Effect of complexation with lanthanide metal ions on the photochromism of (1, 3, 3-trimethyl-5_-hydroxy-6_-formylindoline-spiro 2, 2-[2h] chromene) in different media, Int. J. Photoener. 1–9 (2006).
[41] M.S. Attia, A.O. Youssef, Z.A. Khan, M.N. Abou-Omar, Talanta 186 (2018) 36–43.
[42] M.S. Attia, N.S. Al-Radadi, Biosens. Bioelect. 86 (2016) 413–419.
[43] M.S. Attia, M.H. Khalil, M.S.A. Abdel-Mottaleb, M.B. Lukyanova, Y.A. Alekseenko, B. Lukyanov, Int. J. Photoenergy 2006 (2006) 1–9.
[44] M.S. Attia, A.O. Youssef, A.A. Essawy, Anal. Methods 4 (2012) 2323–2328.
[45] M.S. Attia, K. Ali, M. El-Kemary, W.M. Darwish, Talanta 201 (2019) 185–193.
[46] M.S. Attia, W.H. Mahmoud, A.O. Youssef, M.S. Mostafa, J. Fluoresc. 21 (2011) 2229–2235.
[47] M.S. Attia, M.N. Ramsis, L.H. Khalil, S.G. Hashem, J. Fluoresc. 22 (2012) 779–788.
[48] M.S. Attia, W.H. Mahmoud, M.N. Ramsis, L.H. Khalil, A.M. Othman, S.G. Hashem, M.S. Mostafa, J. Fluoresc. 21 (2011) 1739–1748.
[49] M.S. Attia, A.M. Othman, E. Elraghi, H.Y. Aboul-Enein, J. Fluoresc. 21 (2011) 739–745.
[50] A.A. Elabd, M.S. Attia, J. Lumines. 169 (2016) 313–318.
[51] M.S. Attia, E. Bakir, A.A. Abdel-Aziz, M.S.A. Abdel-Mottaleb, Talanta 84 (2011) 27–33.
[52] M.S. Abdel-Wahed, A.S. El-Kalliny, M.I. Badawy, M.S. Attia, T.A. Gad-Allah, Chem. Eng. J. 382 (2020), 122936.
[53] M.S. Attia, S.A. Elsaadany, K.A. Ahmed, M.M. El-Molla, M.S.A. Abdel-Mottaleb, J. Fluoresc. 25 (2015) 119–125.
[54] S.G. Hashem, M.M. Elsaady, H.G. Afify, M. El-Kemary, M.S. Attia, Talanta 199 (2019) 89–96.

[55] M.S.A. Abdel-Mottaleb, M. Saif, M.S. Attia, M.M. Abo-Aly, S.N. Mobarez, Photochem. Photobio. Sci. 17 (2018) 221–230.
[56] W.E. Omer, M.A. El-Kemary, M.M. Elsaady, A.A. Gouda, M.S. Attia, ACS Omega 5 (2020) 5629–5637.
[57] L.M. Abdullah, M.S. Attia, M.S.A. Abdel-Mottaleb, Egy. J. Chem. 62 (2019) 247–255.
[58] M.S. Attia, A.O. Youssef, A.-S.-S.-H. Elgazwy, S.M. Agami, S.I. Elewa, J. Fluoresc. 24 (2014) 759–765.
[59] M. Abdolrahim, M. Rabiee, S.N. Alhosseini, M. Tahriri, S. Yazdanpanah, I. Tayebi, Development of optical biosensor technologies for cardiac troponin recognition, Anal. Biochem. (2015).
[60] Z. Wu, S.h. Liu, Y. Li, F. Tang, Z. Zhao, Q. Liu, F. Li, Q. Wei, Electrochemiluminescence resonance energy transfer system fabricated by quantum state complexes for cardiac troponin I detection, Sens. Actuat. B 336 (2021), 129733.
[61] D.A. Patel, D.D. Root, Close proximity of myosin loop 3 to troponin determined by triangulation of resonance energy transfer distance measurements, Biochemistry 48(2) (2009) 357–369.
[62] S. Mayilo, M.A. Kloster, M. Wunderlich, A. Lutich, Long-range fluorescence quenching by gold nanoparticles in a sandwich immunoassay for cardiac Troponin T, Nano Lett. 9 (2009) 4558–4563.
[63] International conference on harmonisation of technical requirements for registration of pharmaceuticals for human use, (ICH) Q2 (R1) validation of analytical procedures: text and methodology 1 (2005) 1–15.
[64] J. Malakova, P. Pavek, I. Svecova, P. Zivny, V. Palicka, J. Chromatogr. B 877 (2009) 3226.
[65] M.-L. Järvenpää, K. Kuningas, I. Niemi, P. Hedberg, N. Ristiniemi, K. Pettersson, T. Lövgren, Rapid and sensitive cardiac troponin I immunoassay based on fluorescent europium(III)-chelate-dyed nanoparticles, Clin. Chim. Acta 414 (2012) 70–75.
[66] S. Natarajan and J. Joseph, Signal enhancement using the europium nanoparticle over the organic dye in the quantitative lateral flow immunoassay development for the detection of the cTroponin I, Science Talks 5 (2023) 100151).
[67] K.R. Kim1, H.J. Chun1, Y.D. Han1, K.W. Lee1, D.K. Hong2, K.N. Lee2, H.C. Yoon, A time-resolved fluorescence immunosensing platform for highly sensitive detection of cardiac troponin I, Transducers 2017 (2017) 18–22.
[68] T. Rodrigues, V. Mishyn, A. Bozdogan, Y.R. Leroux, Henri Happy et al., On the detection of cTnI Annals of Clinical and Medical Case Reports 6 (2) (2021) 1–16.
[69] Ka Ram Kim, Yong Duk Han, Hyeong Jin Chun, Kyung Won Lee, Dong-Ki Hong, Kook-Nyung Lee, Hyun C. Yoon, Encapsulation-stabilized, europium containing nanoparticle as a probe for time-resolved luminescence detection of cardiac troponin I, Biosensors 7 (2017) 48.
[70] F. Di Serio, M. Caputo, M. Zaninotto, C. Ottomano, M. Plebani, Evaluation of analytical performance of the Pathfast cardiac troponin I, Clin. Chem. Lab. Med. 47 (7) (2009) 829–833.